arXiv:1303.2272v1 [nucl-th] 9 Mar 2013

Neutrino Oscillations

A.B. Balantekin,[1]
W.C. Haxton[2]

[1]Physics Department, University of Wisconsin, Madison WI 53706 USA
[2]Department of Physics, University of California, and
Lawrence Berkeley National Laboratory, Berkeley, CA 94720

March 12, 2013

Abstract

This review summarizes recent experimental and theoretical progress in determining neutrino mixing angles and masses through neutrino oscillations. We describe the basic physics of oscillation phenomena in vacuum and matter, as well as the status of solar, reactor, atmospheric, and accelerator neutrino experiments that probe these phenomena. The results from current global analyses of neutrino parameters are given. Future efforts that may improve the precision with which these parameters are known or probe new aspects of the neutrino mixing matrix are described.

1 Introduction

The Standard Model (SM) of particle physics provides a renormalizable theory where charged fermions acquire Dirac masses through the Higgs mechanism. In this model the neutrinos stand out, lacking charges or any other additively conserved quantum numbers to distinguish particle and antiparticle, and consequently having the possibility of both Dirac and Majorana masses, yet acquiring neither in the SM. The structure of the SM – the absence of right-handed fields necessary for Dirac masses and of dimensional effective couplings necessary for Majorana masses – eliminates neutrino mass terms. Consequently the discovery 15 years ago of massive neutrinos supports the modern view of the SM as an effective theory, where for example Majorana neutrino masses would arise from the SM's unique dimension-five operator, and thus can be considered the most natural correction to that model. Hence neutrino masses represent an important opportunity to look for extensions of the SM and to determine the scales of the new physics that we now need to add to that model. Experiment has confirmed that there is a hierarchy of neutrino masses, just as there are differences between electron, muon, and tauon masses, though the overall scale of neutrino masses is radically different from that of the charged fermions, below $\sim$ an eV rather than $\gtrsim$ MeV. This has implications for the scale of the new physics. It has also confirmed that there is flavor violation among the neutrinos – the mass and weak interaction eigenstates are different – with the mixing angles being much larger than those found among the quarks. This has provided us with a powerful tool for probing neutrino properties, oscillations that couple the flavors with significant amplitudes.

The discovery of neutrino masses and mixing, as well as the changes in the mixing that accompanies neutrino propagation in matter, has stimulated a great deal of new experimental and theoretical activity.

Neutrino oscillation experiments have provided a reasonably clear picture of neutrino mixing angles and neutrino mass differences, though their are important issues not yet unresolved. Some of the remaining questions can be addressed with neutrino oscillations – e.g., the mass hierarchy, the Dirac CP phase, and the possible existence of additional neutrino generations – and some questions – the absolute scale of neutrino mass, the nature of that mass (its Dirac/Majorana character), and the Majorana CP phases – must be addressed by other techniques. This review summarizes the current status of neutrino oscillation studies and prospects for further exploiting this probe to test neutrino properties.

2 Neutrino mixing and Oscillations

The neutrino mixing matrix defines the relationship between the mass eigenstate and weak (flavor) eigenstate bases,

$$|\nu_{\text{flavor}}\rangle = \mathbf{T}|\nu_{\text{mass}}\rangle. \tag{1}$$

We adopt the following parametrization of the neutrino mixing matrix:

$$\mathbf{T} = \mathbf{T}^{(23)}\mathbf{T}^{(13)}\mathbf{T}^{(12)} = \begin{pmatrix} 1 & 0 & 0 \\ 0 & C_{23} & S_{23} \\ 0 & -S_{23} & C_{23} \end{pmatrix} \begin{pmatrix} C_{13} & 0 & S_{13}e^{-i\delta_{CP}} \\ 0 & 1 & 0 \\ -S_{13}e^{i\delta_{CP}} & 0 & C_{13} \end{pmatrix} \begin{pmatrix} C_{12} & S_{12} & 0 \\ -S_{12} & C_{12} & 0 \\ 0 & 0 & 1 \end{pmatrix} \tag{2}$$

where $C_{ij} = \cos\theta_{ij}$, $S_{ij} = \sin\theta_{ij}$, and δ_{CP} is the CP-violating phase. In writing Eq. (2) we have omitted the two Majorana phases because these play no role in neutrino oscillations. Note that the association of the CP-violating phase with S_{13} is simply a parametrization choice. In fact the CP-violating difference of the neutrino survival probabilities

$$P(\bar{\nu}_\mu \to \bar{\nu}_e) - P(\nu_\mu \to \nu_e), \tag{3}$$

is proportional to a product of the sines of all three mixing angles.

Consider a particular flavor eigenstate, $|\nu_f\rangle = \sum_i T_{fi}|\nu_i\rangle$, created at some point in time by weak interactions, where the indices f and i denote flavor and mass eigenstates respectively. The subsequent propagation of this state is controlled by the free Lagrangian and consequently by the neutrino masses. As the neutrino travels downstream from the source, the different mass eigenstates accumulate phases that depend on their masses, with the differences in these phases governing the beating among the mass eigenstates. If the initial state of definite flavor was created as a three-momentum eigenstate (a simplification, as one should employ wave packets), the amplitude for finding the state in its original flavor at time t and distance ct from the source is

$$A(\nu_f \to \nu_f) = e^{i\vec{p}\cdot\vec{x}} \sum_i \mathbf{T}_{fi} e^{-iE_i t} \mathbf{T}^\dagger_{if}. \tag{4}$$

The time evolution of this state is governed by the $E_i = \sqrt{\vec{p}^2 + m_i^2}$, given that a momentum eigenstate was assumed, which we expand for small neutrino masses as $p + m_i^2/2p$. The flavor of the state thus evolves if some of the m_i^2 differ. The electron neutrino survival probability downstream can be evaluated from Eq. (4),

$$P(\nu_e \to \nu_e) = 1 - \sin^2 2\theta_{13} \left[\cos^2\theta_{12}\sin^2(\Delta_{31}L) + \sin^2\theta_{12}\sin^2(\Delta_{32}L)\right] - \cos^4\theta_{13}\sin^2 2\theta_{12}\sin^2(\Delta_{21}L) \tag{5}$$

where L is the distance traveled ($\hbar = c = 1$) and

$$\Delta_{ij} \equiv \frac{\delta m_{ij}^2}{4E} = \frac{m_i^2 - m_j^2}{4E}. \tag{6}$$

Similar probabilities can be evaluated for new flavors appearing downstream, with the probabilities summing to 1. The mixing angles θ_{ij} and mass differences δm_{ij}^2 (include their signs) can thus be determined from the variation of the neutrino oscillation pattern with distance and beam energy. If the case of oscillations among three light neutrinos, only two of the three δm_{ij}s are independent, as $\delta m_{12} + \delta m_{23} + \delta m_{31} = 0$.

Just as photons traveling through matter propagate according to their index of refraction, neutrinos traveling through matter acquire effective masses due to coherent forward scattering off surrounding particles [1]. The flavor dependence of this phenomenon – ordinary matter contains electrons, but not muons or tauons – can lead to striking effects, enhancing neutrino oscillation probabilities relative to those seen in vacuum [2]. The phenomenon is a familiar one, an adiabatic level crossing, and is particularly dramatic for small mixing angles. For example, an electron neutrino that might be nearly coincident with a light neutrino mass eigenstate in vacuum ($\theta_{12}(\rho = 0) \sim 0$) would be coincident with the local heavy mass eigenstate at sufficiently high density ($\theta_{12}(\rho \to \infty) \to \pi/2$), as the effective mass contribution of the matter overcomes the δm_{21}^2 difference that exists in vacuum. For example, in the Sun the electron neutrinos produced in the high-density solar core could be nearly coincident with the heavy-mass eigenstates. If the neutrino then propagates adiabatically from high density to the vacuum that exists at the solar surface – this requires that the local oscillation length always be small compared to the scale height of solar density changes – the neutrino would then emerge into vacuum on the heavy-mass trajectory, which would be nearly coincident with, say, the muon neutrino. This phenomenon is known as the Mikheyev-Smirnov-Wolfenstein (MSW) effect. The oscillations that occur among three neutrino species in the presence of static matter is governed by the equation

$$i\frac{\partial}{\partial t}\begin{pmatrix}\Psi_e\\ \Psi_\mu\\ \Psi_\tau\end{pmatrix} = \left[\mathbf{T}^{(23)}\mathbf{T}^{(13)}\mathbf{T}^{(12)}\begin{pmatrix}E_1 & 0 & 0\\ 0 & E_2 & 0\\ 0 & 0 & E_3\end{pmatrix}\mathbf{T}^{(12)\dagger}\mathbf{T}^{(13)\dagger}\mathbf{T}^{(23)\dagger} + \begin{pmatrix}V_c + V_n & 0 & 0\\ 0 & V_n & 0\\ 0 & 0 & V_n\end{pmatrix}\right]\begin{pmatrix}\Psi_e\\ \Psi_\mu\\ \Psi_\tau\end{pmatrix}, \tag{7}$$

where the Wolfenstein potentials in charge-neutral and unpolarized matter are given by

$$V_c(\vec{x}) = \sqrt{2}G_F N_e(\vec{x}) \tag{8}$$

for charged-current weak interactions and by

$$V_n(\vec{x}) = -\frac{1}{\sqrt{2}}G_F N_n(\vec{x}) \tag{9}$$

for neutral current interactions. In these equations N_e and N_n are the electron and neutron number densities of the medium, respectively. As an overall phase does not contribute to the interferences, we can take out a term proportional to the identity by defining $V_e = V_c + V_n$, $V_\mu = V_\tau = V_n$, and subtracting $V_\mu\mathbf{1}$ from the second term in Eq. (7). Hence, the term V_n drops out of the MSW equations for active neutrinos – leaving V_c to generate the electron neutrino effective mass in the solar example given above. However, if sterile neutrinos are present, Eq. (7) must be expanded to include the additional neutrino species, and V_n would then contribute to the potential coupling active and sterile neutrinos. Also note that there is a SM loop correction [3]

$$V_\tau - V_\mu = -\frac{3\sqrt{2}G_F\alpha}{\pi\sin^2\theta_W}\left(\frac{m_\tau}{m_W}\right)^2\left\{(N_p + N_n)\log\frac{m_\tau}{m_W} + \left(\frac{N_p}{2} + \frac{N_n}{3}\right)\right\}, \tag{10}$$

where N_p is the proton number density of the medium, m_τ is the tau lepton mass, θ_W is the Weinberg angle, and m_W is the mass of the W-boson. This correction is negligible for the phenomena we consider here, but may be important in core-collapse supernovae. Similarly we will ignore interactions between neutrinos, which again play an important role in supernovae due to the enormous neutrino densities produced by neutrino trapping [4].

Often matter-enhanced neutrino oscillations, Eq. (7), are treated by retaining just two of the three flavors. Indeed if the mixing angle θ_{13} were zero, Eq. (7) can be exactly reduced to a two-dimensional problem [5]. As two-flavor evolution is numerically simpler it is still widely employed. The contribution of the non-zero value of θ_{13} to the electron neutrino survival probability can be obtained using the formula [6, 7]

$$P_{3\times3}(\nu_e \to \nu_e) = \cos^4\theta_{13}(1-4\sin^2\theta_{13}\alpha)\; P_{2\times2}(\nu_e \to \nu_e \text{ with } N_e\cos^2\theta_{13}) + \sin^4\theta_{13}(1+4\cos^2\theta_{13}\alpha) \tag{11}$$

where

$$\alpha = \frac{1}{\Delta_{32}+\Delta_{31}}\sqrt{2}G_F N_e(r=0). \tag{12}$$

(We are envisioning an application to a case like the Sun, where spherical symmetry can be assumed, and thus where densities are a function of the radial coordinate only. Here $r = 0$ is the solar center.) This formula is obtained by expanding the full survival probability as a power series in $\sin\theta_{13}$. One can calculate the survival probability for the two-flavor case in Eq. (11) by solving the equation

$$i\frac{\partial}{\partial t}\begin{pmatrix}\psi_e\\ \psi_x\end{pmatrix} = \begin{pmatrix}\frac{1}{2}\tilde{V}-\Delta_{21}\cos 2\theta_{12} & \frac{1}{2}\Delta_{21}\sin 2\theta_{12}\\ \frac{1}{2}\Delta_{21}\sin 2\theta_{12} & -\frac{1}{2}\tilde{V}+\Delta_{21}\cos 2\theta_{12}\end{pmatrix}\begin{pmatrix}\psi_e\\ \psi_x\end{pmatrix}, \tag{13}$$

where $\tilde{V} = \sqrt{2}G_F N_e(r)\cos^2\theta_{13}$ and $\psi_x = \cos\theta_{23}\psi_\mu - \sin\theta_{23}\psi_\tau$. The MSW level crossing, where the adiabatic condition is most severe, is the point where the diagonal terms are equal to zero.

In some situations the matter basis simplifies the solutions; by making the change of basis

$$\begin{pmatrix}\psi_1(r)\\ \\ \psi_2(r)\end{pmatrix} = \begin{pmatrix}\cos\theta_m(r) & -\sin\theta_m(r)\\ \\ \sin\theta_m(r) & \cos\theta_m(r)\end{pmatrix}\begin{pmatrix}\psi_e(r)\\ \\ \psi_x(r)\end{pmatrix}, \tag{14}$$

the flavor-basis Hamiltonian of Eq. (13) can be instantaneously diagonalized. The cosine of this matter mixing angle is

$$\cos 2\theta_m(r) = -\frac{(2BE-\cos 2\theta_{12})}{\sqrt{(2BE-\cos 2\theta_{12})^2+\sin^2 2\theta_{12}}} \tag{15}$$

where

$$B = \sqrt{2}G_F N_e\cos^2\theta_{13}/\delta m^2_{21}. \tag{16}$$

(This result corresponds to the more familiar two-flavor relationship between flavor and local-mass eigenstates when $\theta_{13} \to 0$.)

Note that matter effects depend on the sign of δm^2, i.e., on the neutrino mass hierarchy. Furthermore, as the matter background is not CP-symmetric (no antiparticles), matter effects induce an effective CP violation. However, in the absence of sterile neutrino mixing, the CP-violating phase δ_{CP} does not impact neutrino oscillations even in the presence of a matter background [8, 9].

3 Measuring θ_{12}: Solar and Reactor Neutrinos

The Sun and about 80% of the visible stars produce their energy by the conversion of hydrogen to helium via

$$2e^- + 4p \to {}^4\text{He} + 2\nu_e + 26.73\ \text{MeV}. \tag{17}$$

Consequently stars, including our Sun, are prodigious sources of neutrinos. This conversion proceeds primarily through the pp chain in lower mass, cooler stars like our Sun, and primarily through the CNO cycles in heavier mass, hotter stars. The pp chain, responsible for $\sim 99\%$ of solar energy production, is

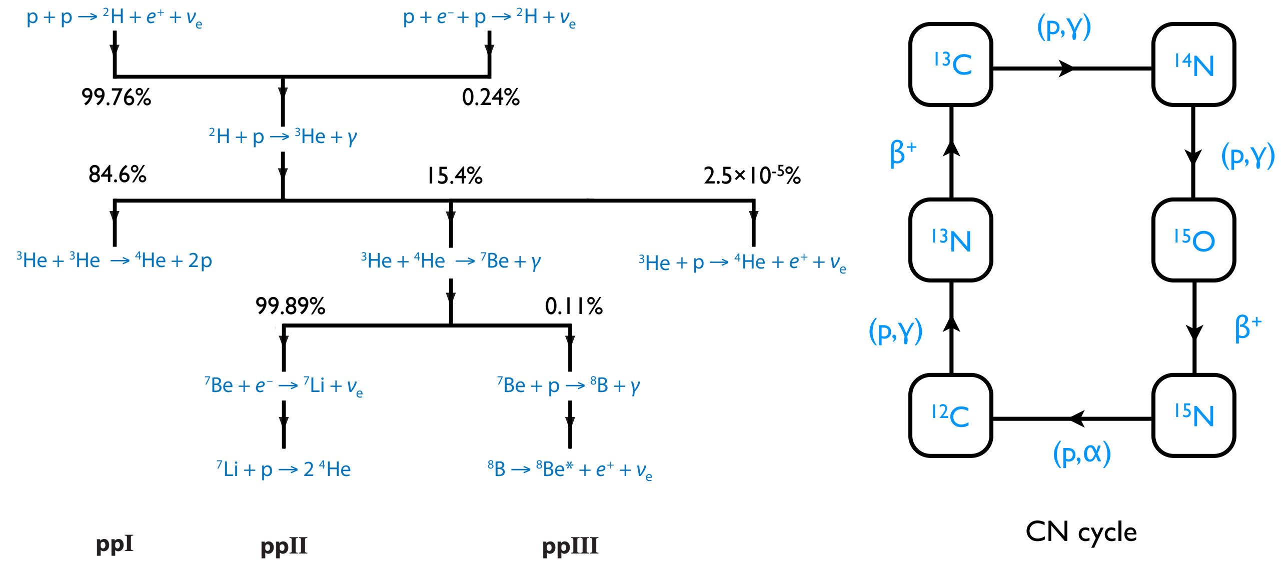
$p + p \rightarrow {}^2H + e^+ + \nu_e$
$p + e^- + p \rightarrow {}^2H + \nu_e$
99.76%
0.24%
${}^2H + p \rightarrow {}^3He + \gamma$
84.6%
15.4%
2.5×10-5%
${}^3He + {}^3He \rightarrow {}^4He + 2p$
${}^3He + {}^4He \rightarrow {}^7Be + \gamma$
${}^3He + p \rightarrow {}^4He + e^+ + \nu_e$
99.89%
0.11%
${}^7Be + e^- \rightarrow {}^7Li + \nu_e$
${}^7Be + p \rightarrow {}^8B + \gamma$
${}^7Li + p \rightarrow 2\,{}^4He$
${}^8B \rightarrow {}^8Be^* + e^+ + \nu_e$
ppI
ppII
ppIII
${}^{13}C$
(p,γ)
${}^{14}N$
β+
(p,γ)
${}^{13}N$
${}^{15}O$
(p,γ)
β+
${}^{12}C$
${}^{15}N$
(p,α)
CN cycle

Figure 1: The left frame shows the three principal cycles comprising the pp chain (ppI, ppII, and ppIII), the neutrinos sources associated with these cycles, and the theoretical branching percentages defining the relative rates of competing reactions, taking from the GS98-SFII SSM [10]. Also shown is the minor branch ^{3}He+p $\rightarrow$ ^{4}He+e$^+$+ν_e, which generates the most energetic solar neutrinos. The right frame shows the CN I cycle, which produces the ^{13}N and ^{15}O neutrinos. Figure from [11].

comprised of three principal cycles, ppI, ppII, and ppIII, each of which is associated with a distinctive neutrino source. The competition among these three cycles in very sensitive to temperature. The CN I cycle contribution to solar energy generation depends on pre-existing C and N to catalyze reactions, and thus is sensitive to metallicity as well as temperature. Despite its minor role in solar energy generation, the CN I cycle produces neutrino fluxes from the β decays of ^{13}C and ^{15}N that are potentially measurable. The reaction chains are depicted in Fig. 1, including pp-chain branching ratios from a recently updated Standard Solar Model (SSM), GS98-SFII [10]. See Ref. [11] for a recent comprehensive review of solar neutrino physics, to supplement the summary provided here.

Pontecorvo first suggested that neutrinos might be detectable by radiochemical means in a large volume of chlorine-bearing liquid (see the reproduction of his original paper in Ref. [12]). This idea was subsequently developed by L. Alvarez and later by R. Davis, Jr. In 1964 Davis and his theoretical colleague J. Bahcall argued in back-to-back Physical Review Letters [13, 14] that a successful solar neutrino experiment could be done, given a sufficient detector volume and a deep underground location to reduce cosmic-ray-associated backgrounds. They gave as the scientific motivation for their proposal "..to see into the interior of a star and thus verify directly the hypothesis of nuclear energy generation..." First results from the Cl detector were reported in 1968 [15], and it soon became apparent that the measured solar neutrino flux was about one third that predicted by the SSM of the time.

The source of this discrepancy was unclear for many years because of the large contribution of the high-energy ^{8}B neutrinos to the Cl capture rate: the flux of these neutrinos is so sensitive to the solar core temperatures that a 5% reduction in that temperature would have brought theory into agreement with measurement. The situation began to clarify around 1990, when three new experiments produced data. The converted proton-decay water Cerenkov detector Kamiokande II reported the results of 450 days of solar neutrino running in 1989, establishing that the ^{8}B flux was $\sim$ 46% the SSM model prediction [16], in approximate agreement with the Davis result. The signal in this detector was the Cherenkov light produced by recoiling electrons after neutrino scattering. This experiment was the first to detect neutrinos in real time and the first to establish their solar origin by correlating the direction of electron scattering events with the position of the Sun. First results from SAGE and GALLEX, radiochemical detectors employing ^{71}Ga as a target because of its low threshold and consequent sensitivity to pp solar neutrinos, were reported in 1991 and 1992, respectively. The 1991 SAGE result, based on the first five extractions of the daughter nucleus ^{71}Ge, was an upper bound on the counting rate of 79 SNU at 90% c.l.[17] (SNU = solar neutrino unit, 10^{-36} captures/target atom/sec). The 1992 GALLEX result, based on an initial 14 extractions, was 83 ± 19 (stat) ± 8 (syst) SNU [18]. Both rates were uncomfortably close to the minimum astronomical value of 79 SNU [19], which assumes only a steady-state Sun and standard-model weak interaction physics. GALLEX and its successor GNO operated until 2003 [20, 21]; SAGE remains an active experiment [22]. Because the chemistry of ^{71}Ge extraction from Ga is considerably more complicated than that of ^{37}Ar extraction from Cl, efforts were made to calibrate the overall efficiency of both Ga experiments with intense ^{51}Cr and ^{37}Ar neutrino sources ($\sim$ 0.5 MCi) [23, 24]. Four such calibration experiments were performed, yielding a weighted average of measured to expected ^{71}Ge of 0.87 ± 0.05 [22]. A counting rate of 66.1 ± 3.1 SNU [22] was obtained by combining all results from SAGE, GALLEX, and GNO through 2009. This rate can be compared to the GS98-SFII SSM prediction of 126.6 ± 4.2 SNU [10].

In the early 1990s, particularly with the uncertainties that accompanied the initial results from Kamioka II and the Ga experiments, no individual experiment required a non-astrophysical solution of the solar neutrino problem. But in aggregate, the Cl, Kamioka II, and Ga experiments indicated a pattern of neutrino fluxes that was not compatible with any adjustment of the SSM. This was pointed out in a series of papers by various authors as the data became more constraining, eventually establishing with a high degree of confidence that the observed rates were inconsistent with the assumptions of a steady-state Sun producing undistorted fluxes of solar neutrinos [25, 26, 27, 28, 29].

These early results combined with the spectacular success of the SSM in another context – reproducing the sound speed profile deduced from helioseismology to sub-1% accuracy throughout much of the solar interior [19] – made a particle-physics solution to the solar neutrino problem more likely. This is turn helped motivate a new generation of spectacularly capable active detectors. These experiments are Super-Kamiokande, a 50-kiloton water Cherenkov detector from which the ^{8}B flux was determined to better than 3%; the Sudbury Neutrino Observatory (SNO), which employed a central 1-kiloton volume of heavy water in order to measure three neutrino reaction channels with different sensitivities to flavor; and Borexino, which uses liquid scintillator, extending real-time, event-by-event counting to low energy fluxes such as the ^{7}Be and pep neutrinos. Both Super-Kamiokande and Borexino continue to operate.

Results from the SNO detector were definitive in proving new particle physics was responsible for the solar neutrino deficit Ray Davis first discovered. Like Super-Kamiokande, SNO was able to detect elastic scattering (ES) events

$$\nu_x + e^- \rightarrow \nu_x + e^- \tag{18}$$

which, due to the charged-current contribution to ν_e scattering, has a relative sensitivity to ν_es and heavy-flavor neutrinos of $\sim$ 7:1. In addition, SNO could detect ν_es through the charged current (CC) reaction

$$\nu_e + d \rightarrow p + p + e^-, \tag{19}$$

by observing the Cherenkov light from the recoiling electron. Unlike the ES case, in the CC reaction the e^- carries away most of the energy release, so that the electron recoil spectrum becomes an important test of the neutrino spectrum. SNO's third reaction was the neutral current (NC) breakup reaction

$$\nu_x(\overline{\nu}_x) + d \rightarrow \nu_x(\overline{\nu}_x) + p + n. \tag{20}$$

This reaction is independent of flavor and thus sensitive to the total flux of neutrinos: by detecting the neutron, one can determine a rate that corresponds to an integral over the neutrino spectrum above the 2.22 MeV deuterium breakup threshold. To exploit this reaction, great care had to be taken to reduce

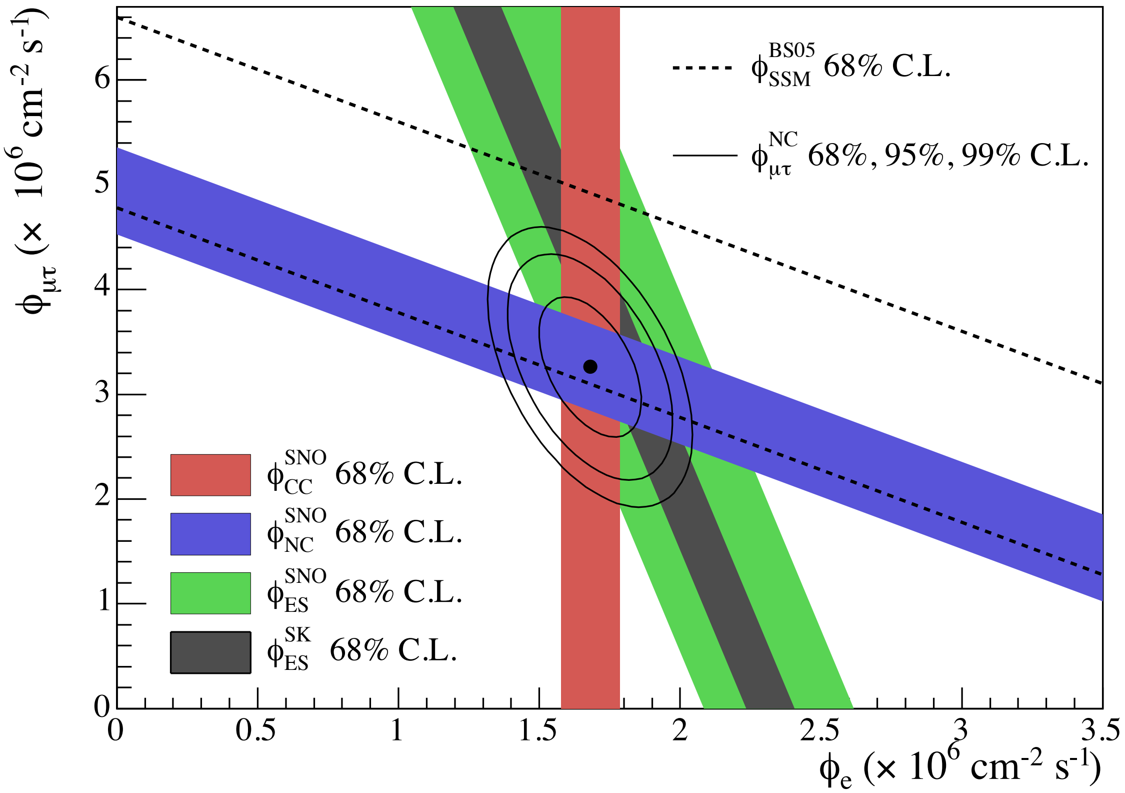

Figure 2: The SNO CC, ES, and NC and Super-Kamiokande ES constraints on the ν_e and $\nu_{\mu\tau}$ components of the ^{8}B flux are shown. The SSM total flux is also shown. All results are all consistent with a terrestrial flux of solar neutrinos that is about one-third ν_es and two-thirds $\nu_{\mu\tau}$ [31]. Reproduced with permission from [32].

background sources of neutrons from natural radioactivity and from cosmic ray muons. SNO's great depth, two kilometers below the surface, was helpful in addressing the latter. The SNO experiment was carried out in three phases in which distinct methods were used in the NC channel, neutron capture on deuterium, on Cl introduced as salt in the heavy water, and in an array of ^{3}He proportional counters constructed in the central detector. The SNO results for the CC, ES, and NC channels, the Super-Kamiokande ES results, and the predictions of the SSM circa 2005 are shown in Fig. 2. The data are consistent, showing that approximately two-thirds of the solar neutrinos arriving at earth are heavy-flavor neutrinos [30, 31]. The total flux is consistent with the SSM, given assigned uncertainties.

Table 1 summarizes the properties of the solar neutrino experiments carried out to date.

The solar neutrino demonstration of neutrino oscillations was confirmed in the KamLAND reactor neutrino experiment [33]. The KamLAND experiment used neutrinos from 55 Japanese nuclear reactors with a flux-weighted average baseline of 180 km, a distance fortuitously appropriate for observing oscillations governed by the solar δm^2_{21}. The KamLAND results provided a precise determination of $\delta m^2_{12} \sim (7.41^{+0.21}_{-0.19}) \times 10^{-5}$ eV^2, eliminating an ambiguity that existed in analyses that included only solar neutrino data: both the LMA (large mixing angle) solution corresponding to $\delta m_{12} \sim 8 \times 10^{-5}$ eV^2 and the LOW solution, $\delta m^2_{12} \sim 10^{-7}$ eV^2, were allowed at 67% c.l., prior to KamLAND measurements. KamLAND results eliminated the LOW solution.

Neutrino propagation in the Sun is influenced by matter, which alters the relationship between the local mass eigenstates, effectively rotating the local mixing angle toward $\pi/2$ with increasing density. The electron neutrino survival probability at Earth, averaged over the solar core production region

Table 1: Solar neutrino experiments.

Experiment	*Type*	*Method*	*Dates*	*Threshold(MeV)*	*Main Fluxes*
Homestake Cl	radiochem	CC	1968-2002	0.811	^{8}B, ^{7}Be
Kamiokande	active	ES	1987-1995	7.0-9.0	^{8}B
SAGE	radiochem	CC	1990-present	0.233	pp, ^{7}Be
GALLEX/GNO	radiochem	CC	1991-2003	0.233	pp, ^{7}Be
Super-Kamiokande	active	ES	1996-present	4.0-7.0	^{8}B
SNO	active	ES/CC/NC	1999-2006	4.0-7.25; 2.22(NC)	^{8}B
Borexino	active	ES	2008-present	~ 0.8	^{7}Be, pep, ^{8}B

(which removes interference terms between the local heavy and light mass eigenstates), is

$$P^D_{2\times 2}(\nu_e \to \nu_e) = \frac{1}{2} + \frac{1}{2}\cos 2\theta_{12} \langle \cos 2\theta_i \rangle_{source}\,(1 - 2P_{hop})\,. \tag{21}$$

Here $\langle \cos 2\theta_i \rangle_{source}$ is the local mixing angle at the point of neutrino production, suitably averaged over the neutrino-producing region of the solar core; the superscript D indicates that the neutrino has been observed during the day, so that matter effects associated with passage through the earth play no role; and the subscript 2×2 indicates that subdominant oscillations involving the third flavor have been neglected. P_{hop} is the probability that the neutrino hops from the heavy-mass trajectory to the light-mass trajectory on traversing the level-crossing point [34, 35]. This accounts for possible non-adiabatic behavior: if the density in this region is treated linearly, one finds

$$P_{hop} = e^{-\pi\gamma_c/2} \tag{22}$$

where γ_c is proportional to the ratio of the Sun's density scale height to the local oscillation length at the crossing point. (Thus large γ_c corresponds to small changes in the solar density over an oscillation length, the adiabatic limit where $P_{hop} \to 0$.)

Solar neutrinos detected at night go through the Earth, hence they would feel additional matter effects [36]. The night-time solar electron neutrino survival probability, averaged over the Earth-Sun distance, is given by [37, 38]

$$P^N_{2\times 2}(\nu_e \to \nu_e) = \frac{1}{2} + \frac{1}{2}\langle \cos 2\theta_i \rangle_{source}\,(1 - 2P_{hop}) \cos 2\theta_e \cos 2(\theta_e - \theta_{12}) \tag{23}$$

where θ_e is the matter mixing angle inside the Earth. In writing Eq. (23), matter density in the mantle of the Earth is assumed to be constant. The day-night asymmetry A is defined as

$$\frac{A}{2} = \frac{P^N - P^D}{P^N + P^D}. \tag{24}$$

The terrestrial matter effects on solar neutrinos that can generate day/night differences are quite small: based on current neutrino parameters obtained from global analyses, a $\sim 3\%$ day-night effect is expected in ES measurements of the ^{8}B spectrum. The latest available Super-Kamiokande results remain consistent with no effect at 2.6 σ [39], though it is quite possible that with the data now being accumulated in Super-Kamiokande IV low-threshold running, this conclusion may change. The corresponding SNO result is less restrictive, consistent with the null hypothesis of no day/night effects at 61% c.l. [31]. The predicted day/night effect in Borexino is tiny, consistent with the collaboration's determination A = 0.001 ± 0.012 (stat) ± 0.007 (syst) [40]. (The absence of day/night effects in Borexino's ^{7}Be flux measurement is an alternative means of eliminating the LOW solution.)

In contrast, matter effects associated with passage through the Sun are large, with the additional suppression being substantial for the higher energy ^{8}B neutrinos. Because matter effects either increase of decrease the local splitting between the mass eigenstates, depending on the hierarchy, solar matter effects allow one to establish that δm^2_{21} is positive ($m_2 > m_1$). Consequently B of Eq. (16) is positive. When one uses neutrino oscillation parameters taken from current global analyses, one finds that low-energy solar neutrino fluxes (pp, pep, ^{7}Be) reside in a region where vacuum effects are dominant,

$$P_{\nu_e}^{\mathrm{vaccum}} \sim 1 - \frac{1}{2}\sin^2 2\theta_{12} \sim 0.57 \tag{25}$$

while oscillation probabilities for the high-energy portion of the ^{8}B neutrino spectrum measured by SNO and Super-Kamiokande are substantially affected by matter

$$P_{\nu_e}^{\mathrm{high\ density}} \to \sin^2\theta_{12} \sim 0.31. \tag{26}$$

These expectations are clearly apparent in the data: the pp flux determined in luminosity-constrained global analyses and the ^{7}Be and pep fluxes determined by Borexino [41, 42] all show the expected turn-up in P_{ν_e} at low E_ν. (See Fig. 3.)

One of the goals of both SNO (CC/ES) and Super-Kamiokande (ES) has been to see the matter effects imprinted on the scattered electrons. SNO's low-energy-threshhold (LET) analysis [31] and Super-Kamiokande IV running both employ total-energy thresholds of $\sim$ 4.0 MeV. This provides sensitivity to a region of the spectrum where the matter-to-vacuum transition might become apparent. The P_{ν_e}s deduced from the SNO LET analysis are included in Fig. 3. While remaining consistent with global analysis predictions, the best fit is trending away from expectations.

The three-flavor analysis based on all solar data supplemented by KamLAND yields [31]

$$\sin^2\theta_{12} = 0.308 \pm 0.014 \quad \delta m^2_{21} \sim (7.41^{+0.21}_{-0.19}) \times 10^{-5}\mathrm{eV}^2 \quad \sin^2\theta_{13} = 0.025^{+0.018}_{-0.015} \tag{27}$$

These results are in excellent agreement with the global analysis that takes into account all neutrino data, including beam experiments and new reactor experiments. The Bari [43] and Valencia [44] analyses yield, respectively,

$$\sin^2\theta_{12} = \begin{cases} 0.306^{+0.018}_{-0.016} \\ \\ 0.319^{+0.016}_{-0.018} \end{cases} \qquad \delta m^2_{21} \sim \begin{cases} (7.54^{+0.26}_{-0.22}) \\ \\ (7.62^{+0.19}_{-0.19}) \end{cases} \times 10^{-5}\mathrm{eV}^2 \qquad \sin^2\theta_{13} = \begin{cases} 0.0243^{+0.0025}_{-0.0027} \\ \\ 0.0248^{+0.0028}_{-0.0030} \end{cases} \tag{28}$$

The solar neutrino analysis supplemented by KamLAND produces a best-value estimate of θ_{13} that is in very good agreement with the Bari and Valencia results. However, the global analyses provide a more certain determination of θ_{13}: this reflects the impact of the recent Daya Bay, RENO, and Double Chooz reactor experiments, which tightened the error bars on θ_{13} by almost an order of magnitude. We discuss these experiments in Sec. 5.

The original goal of solar neutrino spectroscopy was to use neutrinos to test the hypothesis that the Sun is powered by the pp chain and to measure the solar core temperature to high accuracy. This program was delayed by the long effort to identify the origin of the solar neutrino problem and then to accurately determine the parameters governing neutrino oscillations. Consequently today, given the few-percent determinations made of the relevant mixing angles and δm^2_{12}, it has finally become possible to use neutrinos as quantitative astrophysical probes of the Sun and the SSM. In addition to weak interaction uncertainties, the SSM depends on the accuracy with which an additional $\sim$ 20 input parameters are known. These parameters are associated with SSM's nuclear and atomic physics and with properties such as the Sun's initial metallicity, mass, age, luminosity, and the diffusion coefficient. Decades of laboratory and theoretical work on the nuclear and atomic physics input has helped make

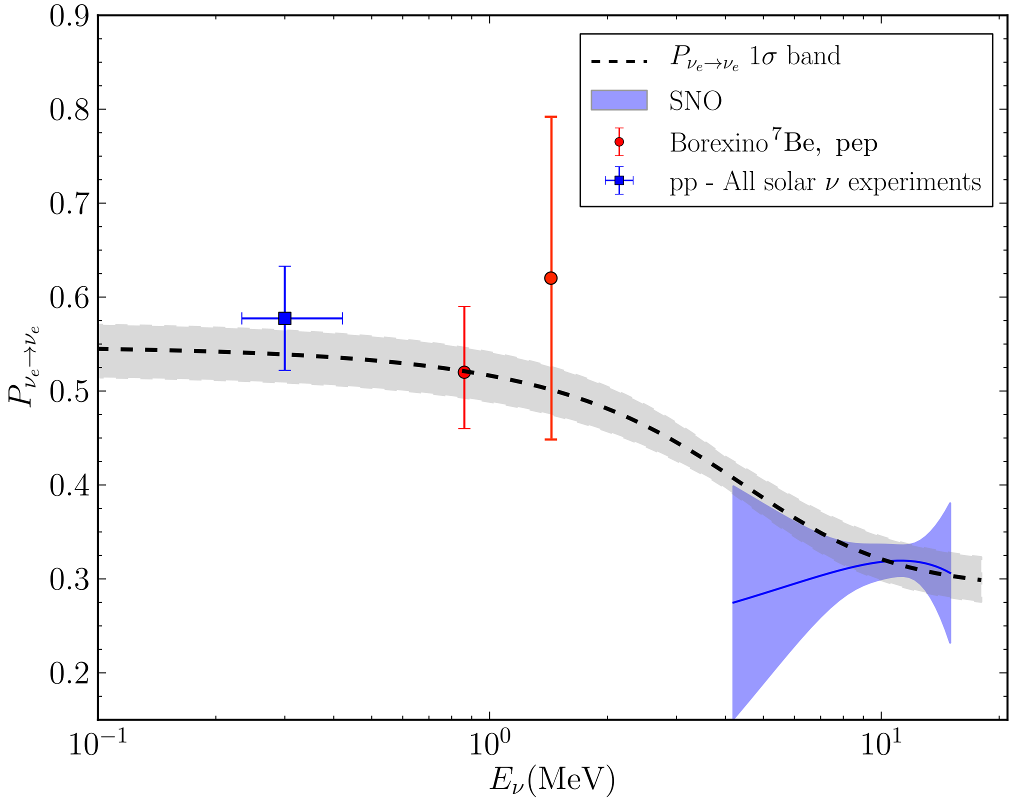

Figure 3: Global analysis pp, Borexino ^{7}Be and pep, and SNO LETA ^{8}B deduced survival probabilities P_{ν_e}. Figure from [11], which was adapted from [31, 42].

the SSM a predictive model, where output uncertainties are known. The laboratory astrophysics of the SSM was advanced by community efforts like that leading to the analysis of cross sections and S-factors published in 1998 [47] (Solar Fusion I). The key uncertainties identified in that analysis led to a decade of further work on critical cross sections, such as that for ^{7}Be(p,γ), and to the recent re-evaluation of cross sections summarized in [48] (Solar Fusion II). Current SSM predictions of neutrino and helioseismic observables have uncertainties based on evaluated input laboratory data. Discrepancies in SSM predictions that significantly exceed model uncertainties could indicate problems with the underlying astrophysics assumptions of the SSM.

The key discrepancy in current SSM predictions is associated with its initial metallicity (abundances of elements heavier than hydrogen and helium). The overall solar metallicity scale is usually determined from analyses of solar photo-absorption lines. Recently more realistic models of the photosphere were constructed to account for its dimensionality and granularity, effects ignored in traditional 1D slab models. When applied to the photospheric data, these new models yield an abundance ratio of metals to hydrogen $(Z/X)_\odot = 0.0178$ [49], compared to the previously accepted value of $(Z/X)_\odot = 0.0229$ [50]. Recent SSM calculations have been carried out for both metallicities [10], while also incorporating the new results from Solar Fusion II. The helioseismic predictions of the low-metallicity SSM are in significant disagreement with observation. The neutrino flux predictions of both models are in reasonable agreement with the data, though it is apparent that a solar core metallicity set to the average of the low- and high-metallicity models would improve the agreement.

This has opened up two directions of study. First, one of the central assumptions of the SSM is that the Sun was homogeneous at the start of the main sequence. There is little observational support for this assumption, given that it is known, late in the evolution of the solar disk, that the process of planetary formation scoured 50-90 $M_\oplus$ of excess metal from the disk. New solar models have been built to take account of the possible accretion of metal-depleted gas onto the proto-Sun, late in its evolution when such accretion would alter convective-zone abundances but not affect the core. It has been found that both solar neutrino and helioseismic data severely constrain such accreting models [10]. Second, the volatile elements CNO play a key role in the solar abundance problem. The SSM produces about 1% of its energy through the CN cycle, yielding significant fluxes of ^{13}N and ^{15}O solar neutrinos. It has been shown, because of the CN cycle's additional linear dependence on the abundance of C+N (these metals catalyze the proton burning), that the C+N abundance of the solar core could be determined to an accuracy of about 10% from the CN neutrino fluxes [51]. This would be very significant given the current 30+% discrepancy between the low- and high-metallicity SSMs. The CN neutrinos can be measured in very deep scintillation detectors such as SNO+, and possibly also in shallower detectors such as Borexino, if strategies for suppressing cosmic-ray muon backgrounds can be further developed.

There are other gaps in our program of solar neutrino spectroscopy. While the pp flux is tightly constrained by the solar luminosity constraint, given existing ^{7}Be and ^{8}B neutrino flux measurements, this constraint itself should be checked: are the Sun's neutrino and photon lumninosities consistent, as predicted in steady-state solar models? Recently the Borexino collaboration succeeded in detecting the pep neutrinos [42], though the accuracy of the measurement is so far limited. This flux should track that of the low-energy pp neutrinos, the dominant solar neutrino flux arising directly from p+p fusion. While the pp flux is constrained by the results from the Ga experiments, no real-time detection has been made. The relation between the photon and neutrino luminosities in steady-state models is [52]

$$\frac{L_\odot}{4\pi d^2} = \sum_i \left(Q - \langle E\rangle\right)_i \phi_i, \tag{29}$$

where d is the average Sun-Earth distance (1 a.u.), Q is the energy released in the nuclear reactions, $\langle E\rangle$ is the average energy loss by neutrinos, and ϕ_i is the neutrino flux at earth, coming from the reaction of type i. (There are corrections to this equation due to the necessary inequalities between different fluxes to take into account the order in which nuclear reactions take place [53, 29]). A test of this relation would require a precise measurement of both the pp- and CNO-chain neutrino fluxes. Such a test would place stringent limits on new neutrino species, while also checking the assumption of steady-state solar burning.

4 Measuring θ_{23}: Atmospheric and Accelerator Neutrinos

The hadronic cosmic ray flux incident on Earth is dominated by energetic protons with fewer numbers of heavy nuclei. When the primary cosmic rays collide with the oxygen and nitrogen in Earth's atmosphere they produce secondary pions, kaons, and muons. Atmospheric neutrinos come from the decay of these secondaries. For energies less than 1 GeV all these secondaries decay in the atmosphere

$$\begin{aligned} \pi^\pm(K^\pm) &\rightarrow \mu^\pm + \nu_\mu(\overline{\nu}_\mu), \\ \mu^\pm &\rightarrow e^\pm + \nu_e(\overline{\nu}_e) + \overline{\nu}_\mu(\nu_\mu). \end{aligned} \tag{30}$$

Consequently one expects the ratio

$$r = (\nu_e + \overline{\nu}_e)/(\nu_\mu + \overline{\nu}_\mu) \tag{31}$$

to be approximately 0.5 in this energy range. This relationship can be checked as a function of distance up to $\sim$ 13000 km, by observing atmospheric neutrinos in a deep detector as a function of zenith angle. It has been customary to use a ratio-of-ratios

$$R = \frac{[(\nu_e + \overline{\nu}_e)/(\nu_\mu + \overline{\nu}_\mu)]_{\rm data}}{[(\nu_e + \overline{\nu}_e)/(\nu_\mu + \overline{\nu}_\mu)]_{\rm Monte\ Carlo}} \tag{32}$$

in this check, normalization the measured r to a Monte Carlo calculation of the ratio assuming no oscillations but including corrections such as geomagnetic effects on the cosmic ray flux.

Early atmospheric neutrino experiments were inconsistent with one another, with some finding $R \sim 1$ while others finding diminished values. Significant indications of an anomaly came from the IMB [54] and Kamiokande [55] detectors. IMB first noticed a possible deficit of neutrino-induced muon events in 1986, while Kamiokande established a deficit in excess of 4σ by 1988. By 1998 the anomaly was also apparent in data taken from the Soudan detector and from Super-Kamiokande [56].

In early experiments it was difficult to adequately explore R because the lack of statistics prevented a detailed analysis as a function of zenith angle. This changed with the construction of Super-Kamiokande, which provided a fiducial volume of $\sim$ 20 ktons. In an initial analysis the Super-Kamiokande Collaboration found

$$R = \begin{cases} 0.61 \pm 0.03(\mathrm{stat}) \pm 0.05(\mathrm{sys}) & \mathrm{sub-GeV\ events,\ fully\ contained} \\ 0.66 \pm 0.05(\mathrm{stat}) \pm 0.08(\mathrm{sys}) & \mathrm{multi-GeV\ events,\ fully\ or\ partially\ contained} \end{cases} \tag{33}$$

The 1998 Super-Kamiokande analysis, based on 33 kton-years of data, showed a zenith-angle dependence for R inconsistent with theoretical calculations of the atmospheric flux, in the absence of oscillations. The distance-dependent muon deficit was consistent with oscillations governed by neutrino mass differences within the range $5 \times 10^{-4}\mathrm{eV}^2 < |\delta m^2_{32}| < 6 \times 10^{-3}\mathrm{eV}^2$ [56]. This differed from that later determined for solar neutrinos. The collaboration concluded that the measurements were consistent with the two-flavor oscillation $\nu_\mu \rightarrow \nu_\tau$, providing evidence for massive neutrinos [56].

Super-Kamiokande I collected $\sim$ 15,000 atmospheric neutrino events over approximately five years of running. The collaboration's zenith-angle analysis of the data placed the first oscillation minimum at $L/E \sim 500$ km/GeV, so that $L_0 \sim 1000$ km for a 1 GeV muon neutrino. Results based on 3903 days of data from Super-Kamiokande I-IV, including 1097 days from the current phase IV, were incorporated

Table 2: Values of $\sin^2 2\theta_{13}$ measured at various experiments. The value quoted for the MINOS experiment corresponds to $2\sin^2\theta_{23}\sin^2 2\theta_{13}$.

Experiment	**Measured** $\sin^2 2\theta_{13}$
Daya Bay [71]	$0.089 \pm 0.010(\text{stat}) \pm 0.005(\text{syst})$
RENO [70]	$0.113 \pm 0.013(\text{stat}) \pm 0.019(\text{syst})$
Double Chooz [68]	$0.109 \pm 0.030(\text{stat}) \pm 0.025(\text{syst})$
T2K (assuming $\theta_{23} = \pi/4$) [72]	$0.104^{+0.060}_{-0.045}$
MINOS [73] (see note)	$+0.041^{-0.047}_{+0.031}$ (normal) $0.079^{+0.071}_{-0.053}$ (inverted)

in a three-flavor analysis in which $\sin^2\theta_{13}$ was set to 0.025, based on Daya Bay, RENO, and Double Chooz results. The analysis yielded [57, 58]

$$\begin{array}{rlrr} \text{Normal hierarchy :} & \delta m^2_{32} = & (2.66^{+0.15}_{-0.40}) \times 10^{-3}\text{eV}^2 & (1\sigma) \\ & \sin^2\theta_{23} = & 0.425^{+0.194}_{-0.034} & (90\%\text{c.l.}) \\ \text{Inverted hierarchy :} & \delta m^2_{32} = & (2.66^{+0.17}_{-0.23}) \times 10^{-3}\text{eV}^2 & (1\sigma) \\ & \sin^2\theta_{23} = & 0.575^{+0.055}_{-0.182} & (90\%\text{c.l.}) \end{array}$$

The significant difference between the normal- and inverted-hierarchy best values for $\sin^2\theta_{23}$ reflects the flatness of the χ^2 fit around $\sin^2\theta_{23} \sim 0.5$, with shallow local minima appearing above and below this value.

Accelerator experiments were conducted by the K2K [59] and MINOS [60, 61] collaborations, with baselines designed to be sensitive to the δm^2_{32} scale probed with atmospheric neutrinos. The MINOS beam-neutrino analysis, which includes atmospheric neutrino data from that detector, determined $|\delta m^2_{32}| = 2.39^{+0.09}_{-0.10}$ eV^2 [62], a value consistent with the somewhat broader range allowed by the atmospheric results. The sign of δm^2_{32} has not been determined, though one can see from the results above that there is some sensitivity to the hierarchy in atmospheric neutrino fits. There are several pending proposals to determine the hierarchy: new, long-baseline neutrino beam experiments (some of these depend on joint analyses of beam and atmospheric neutrino data), high-density arrays to enhance the sensitivity of large detectors like IceCube to atmospheric neutrinos, and new reactor-neutrino experiments with very large detectors to increase sensitivity to subdominant oscillations.

5 Measuring θ_{13}: Reactor and Accelerator Neutrinos

Initial comparisons of the solar neutrino and KamLAND reactor neutrino experiments revealed hints of a non-zero value of θ_{13} [63, 64]. The solar neutrino+KamLAND analysis performed by the KamLAND Collaboration in 2010 yielded $\sin^2\theta_{13} = 0.020^{+0.16}_{-0.16}$ [65], with a nonzero value suggested at 79% c.l. Indications of electron neutrino appearances from accelerator-produced off-axis muon neutrinos in the T2K [66] and MINOS [67] experiments also suggested relatively large values of θ_{13}. In 2012 the Double Chooz reactor collaboration announced data that suggested a nonzero value for $\sin^2 2\theta_{13}$ at 94.6% c.l. [68], followed in quick succession by definitive results from the Daya Bay [69] and RENO collaborations [70] . The various determinations of $\sin^2 2\theta_{13}$ are summarized in Table 2.

Reactor experiments are disappearance experiments, with θ_{13} determined from the magnitude of the electron antineutrino flux loss with distance. The disappearance probability, taken from Eq. (5), is

$$1-P(\nu_e \to \nu_e) = \sin^2 2\theta_{13}\left[\cos^2\theta_{12}\sin^2(\Delta_{31}L) + \sin^2\theta_{12}\sin^2(\Delta_{32}L)\right] + \cos^4\theta_{13}\sin^2 2\theta_{12}\sin^2(\Delta_{21}L). \quad (34)$$

If the experiment is done close to the reactor, $\Delta_{21}L \sim 0$ so that the "solar" oscillation represented by the second term can be ignored. Using the fact $\Delta_{32} \sim \Delta_{31}$, suggested by the solar neutrino experiments, one obtains the disappearance probability

$$1 - P(\nu_e \to \nu_e) = \sin^2 2\theta_{13} \sin^2(\Delta_{31} L). \tag{35}$$

Consequently the very short-baseline reactor neutrino experiments, such as Daya Bay, Double Chooz, and RENO, unambiguously measure θ_{13}, requiring no knowledge of other neutrino mixing angles or the mass hierarchy. Furthermore, the multiple detector configurations currently employed in the Daya Bay and RENO experiments also minimize the effects of reactor neutrino spectrum uncertainties.

The situation is rather different for longer-baseline experiments searching for the appearance of electron neutrinos in a flux of muon neutrinos. For longer baselines neutrinos travel trough the Earth, hence matter effects need to be included. The resulting rather complicated expressions, which depend on many of the neutrino parameters, can be calculated in a series expansion [74]. The appropriate appearance probability in the lowest order is given by

$$P(\nu_\mu \to \nu_e) \sim \frac{\sin^2 2\theta_{13} \sin^2 \theta_{23}}{(1 - G_F N_e/\sqrt{2}\Delta_{31})^2} \sin^2 \left[\left(\Delta_{31} - \frac{G_F N_e}{\sqrt{2}} \right) L \right] + \mathcal{O}(g), \tag{36}$$

where

$$g = \frac{\delta m^2_{21}}{\delta m^2_{31}} \sim 0.03. \tag{37}$$

The next order correction in g to the electron neutrino appearance probability brings in an additional dependence on the CP-violating phase in the neutrino mixing matrix. The denominator of the term multiplying the oscillating term in Eq. (36) depends on the sign of δm^2, i.e. the mass hierarchy of the neutrinos. Consequently, appearance experiments such as T2K [72] and MINOS [73] cannot disentangle θ_{13} from other observables such as the mass hierarchy, θ_{23}, and the CP-violating phase. Note that an intermediate-baseline ($L \sim 60$ km) reactor antineutrino experiment will also have some sensitivity to the neutrino mass hierarchy [75].

6 Final Remarks

The puzzle that arose from early solar neutrino measurements had an interesting resolution, still incomplete. We have reviewed what has been learned in the past 15 years about the properties of neutrinos from oscillations in vacuum and in matter, using astrophysical neutrino sources and terrestrial beams. A great deal of progress has been made, with three mixing angles and two mass differences now accurately determined, and with the sign of δm^2_{12} deduced the effects of solar matter on solar neutrino oscillations. Yet there are several important properties of the light neutrinos that we have not yet been able to determine: the overall scale of the neutrino masses, the mass hierarchy, the Dirac CP-violating phase in the mixing matrix, and neutrino charge-conjugation properties. We have the tools to make further progress. Long-baseline neutrino beam oscillation experiments could distinguish between the normal and inverted mass patterns and determine the CP phase. As we have noted, there may be alternative strategies in which reactor and atmospheric neutrino sources are exploited to probe the neutrino mass hierarchy. A variety of cosmological tests are sensitive to the absolute scale of neutrino mass: the distinctive imprint of neutrino mass on the growth of large-scale structure, affecting both the scale and red-shift dependence of that growth, produces changes in the power spectrum that are roughly an order of magnitude larger than one might naively guess, based on the contribution of neutrinos to the mass density. There are a variety of ongoing projects to improve laboratory sensitivity to neutrino mass, such as the high-sensitivity spectrometer KATRIN for measuring tritium beta decay and the MARE micro-calorimeters for measuring ^{187}Re beta decay, as well as new technologies for overcoming resolution challenges, such as the Project 8 extension to KATRIN. Finally, the exciting question of whether

Nature exploits the neutrino's unique Majorana mass mechanism is stimulating next-generation efforts in double beta decay. As progress is made on all of these fronts, neutrino oscillations will remain one of our most important and most versatile tools from probing the new properties of neutrinos, and thus for seeking new physics beyond the SM.

This work of ABB was supported in part by the U.S. National Science Foundation Grant No. PHY-1205024 (Wisconsin) and the University of Wisconsin Research Committee through funds granted by the Wisconsin Alumni Research Foundation. The work of WCH was supported in part by the US DOE under de-sc00046548 (UC Berkeley) and DE-AC02-98CH10886 (LBL), and by the UC Office of the President.

References

[1] L. Wolfenstein, *Phys. Rev.* D 17 (1978) 2369

[2] S. P. Mikheyev and A. Y. Smirnov, *Sov. J. Nucl. Phys.* 42 (1985) 913 [*Yad. Fiz.* 42 (1985) 1441]

[3] F. J. Botella, C. S. Lim and W. J. Marciano, *Phys. Rev.* D 35 (1987) 896

[4] A.B. Balantekin and G.M. Fuller, contribution to this volume.

[5] A. B. Balantekin and G. M. Fuller, *Phys. Lett.* B 471 (1999) 195

[6] G.L. Fogli, E. Lisi and A. Palazzo, *Phys. Rev.* D 65 (2002) 073019

[7] A. B. Balantekin, *J. Phys. Conf. Ser.* 337 (2012) 012049

[8] E. Kh. Akhmedov, C. Lunardini, and A. Yu. Smirnov, *Nucl. Phys.* B 643 (2002) 339

[9] A. B. Balantekin, J. Gava and C. Volpe, *Phys. Lett.* B 662 (2008) 396

[10] A. M. Serenelli, W. C. Haxton, and C. Peña-Garay, *Astroph. J.* 743 (2011) 24

[11] W. C. Haxton, R. G. Hamish Robertson and A. M. Serenelli, to appear in *Ann. Rev. Astron. Astrophys.* (2013)

[12] B. Pontecorvo, *Camb. Monogr. Part. Phys. Nucl. Phys. Cosmol.* 1 (1991) 25

[13] J. N. Bahcall, *Phys. Rev. Lett.* 12 (1964) 300

[14] Raymond Davis, Jr., *Phys. Rev. Lett.* 12 (1964) 303

[15] R. Davis, Jr., D. S. Harmer and K. C. Hoffman, *Phys. Rev. Lett.* 20 (1968) 1205

[16] K. S. Hirata *et al.* [KAMIOKANDE-II Collaboration], *Phys. Rev. Lett.* 63 (1989) 16

[17] SAGE Collaboration, A. I. Abazov et al., *Phys. Rev. Lett.* 67 (1991) 3332

[18] GALLEX Collaboration, P. Anselmann et al., *Phys. Lett.* B 285 (1992) 376

[19] J. N. Bahcall, *Neutrino Astrophysics.* Cambridge University Press (1989).

[20] W. Hampel *et al.* [GALLEX Collaboration], *Phys. Lett.* B 447 (1999) 127

[21] M. Altmann *et al.* [GNO Collaboration], *Phys. Lett.* B 616 (2005) 174

[22] J. N. Abdurashitov *et al.* [SAGE Collaboration], *Phys. Rev.* C 80 (2009) 015807 and *Phys. Rev.* C 60 (1999) 055801

[23] J. N. Abdurashitov *et al.* [SAGE Collaboration], *Phys. Rev.* C 59 (1999) 2246

[24] W. Hampel *et al.* [GALLEX Collaboration], *Phys. Lett.* B 420 (1998) 114

[25] N. Hata and P. Langacker, *Phys. Rev.* D 48 (1994) 2937

[26] S. J. Parke, *Phys. Rev. Lett.* 74 (1995) 839

[27] M. White, L. Krauss, and E. Gates, *Phys. Rev. Lett.* 70 (1993) 375

[28] N. Hata, S. Bludman, and. P. Langacker, *Phys. Rev.* D 49 (1994) 3622

[29] K. M. Heeger and R. G. H. Robertson, *Phys. Rev. Lett.* 77 (1996) 3720

[30] Q. R. Ahmad *et al.* [SNO Collaboration], *Phys. Rev. Lett.* 87 (2001) 071301

[31] B. Aharmim *et al.* [SNO Collaboration], *Phys. Rev.* C 87 (2013) 015502 and *Phys. Rev.* C 81 (2010) 055504

[32] B. Aharmim *et al.* [SNO Collaboration], *Phys. Rev.* C 72 (2005) 055502

[33] S. Abe *et al.* [KamLAND Collaboration], *Phys. Rev. Lett.* 100 (2008) 221803

[34] W. C. Haxton, *Phys. Rev. Lett.* 57 (1986) 1271

[35] S. J. Parke, *Phys. Rev. Lett.* 57 (1986)) 1275

[36] J. N. Bahcall and P. I. Krastev, *Phys. Rev.* C 56 (1997) 2839

[37] M. C. Gonzalez-Garcia, C. Peña-Garay, Y. Nir and A. Y. Smirnov, *Phys. Rev.* D 63 (2001) 013007

[38] H. Minakata and C. Peña-Garay, *Ad. High Energy Phys.* 2012 (2012) 349686

[39] M. Smy, to appear in the Proc. Neutrino 2012 (2013).

[40] G. Bellini *et al.* [Borexino Collaboration], *Phys. Lett.* B 707 (2012) 22 .

[41] G. Bellini *et al.* [Borexino Collaboration], *Phys. Rev. Lett.* 107 (2011) 141302

[42] G. Bellini *et al.* [Borexino Collaboration], *Phys. Rev. Lett.* 108 (2012) 051302

[43] G. L. Fogli *et al.*, *Phys. Rev.* D 86 (2012) 013012

[44] D. V. Forero, M. Tórtola, and J. W. F. Valle, *Phys. Rev.* D 86 (2012) 073012

[45] A. B. Balantekin and A. Malkus, *Phys. Rev.* D 85 (2012) 013010

[46] K. Abe *et al.* [Super-Kamiokande Collaboration], *Phys. Rev.* D 83 (2011) 052010

[47] E. G. Adelberger *et al.*, *Rev. Mod. Phys.* 70 (1998) 1265

[48] E. G. Adelberger *et al.*, *Rev. Mod. Phys.* 83 (2011) 195

[49] M. Asplund, N. Grevesse, A. J. Sauval and P. Scott, *Ann. Rev. Astron. Astrophys.* 47 (2009) 481

[50] N. Grevesse and A. J. Sauval, *Space Sci. Rev.* 85 (1998) 161

[51] W. C. Haxton and A. M. Serenelli, *Astrophys. J.* 687 (2008) 678 ; A. Serenelli, C. Peña-Garay, and W. C. Haxton, *Phys. Rev.* D 87 (2013) 043001

[52] M. Spiro and D. Vignaud, *Phys. Lett.* B 242 (1990) 279 .

[53] J. N. Bahcall and P. I. Krastev, *Phys. Rev.* D 53 (1996) 4211

[54] T. J. Haines *et al., Phys. Rev. Lett.* 20 (1986) 1986 ; D. Casper *et al.*, *Phys. Rev. Lett.* 66 (1991) 2561

[55] K. S. Hirata *et al.*, *Phys. Lett.* B 205 (1988) 416

[56] Y. Fukuda *et al.* [Super-Kamiokande Collaboration], *Phys. Rev. Lett.* 81 (1998) 1562

[57] Y. Itow, talk presented at Neutrino 2012.

[58] Y. Ashie *et al.* [Super-Kamiokande Collaboration], *Phys. Rev.* D 71 (2005) 112005

[59] M. H. Ahn *et al.* [K2K Collaboration], *Phys. Rev.* D 74 (2006) 072003

[60] P. Adamson *et al.* [MINOS Collaboration], *Phys. Rev. Lett.* 108 (2012) 191801

[61] P. Adamson *et al.* [MINOS Collaboration], *Phys. Rev.* D 86 (2012) 052007

[62] R. Nichol [MINOS Collaboration], talk presented at Neutrino 2012.

[63] A. B. Balantekin and D. Yilmaz, *J. Phys. G* 35 (2008) 075007

[64] G. L. Fogli, E. Lisi, A. Marrone, A. Palazzo and A. M. Rotunno, *Phys. Rev. Lett.* 101 (2008) 141801

[65] A. Gando. *et al.* [KamLAND Collaboration], *Phys. Rev.* D 83 (2011) 052002 .

[66] K. Abe *et al.* [T2K Collaboration], *Phys. Rev. Lett.* 107 (2011) 041801

[67] P. Adamson *et al.* [MINOS Collaboration], *Phys. Rev. Lett.* 103 (2009) 261802 and *Phys. Rev. Lett.* 107 (2011) 181802

[68] Y. Abe *et al.* [Double Chooz Collaboration], *Phys. Rev. Lett.* 108 (2012) 131801

[69] F. P. An *et al.* [DAYA-BAY Collaboration], *Phys. Rev. Lett.* 108 (2012) 171803 and *Nucl. Instrum. Meth. A* 685 (2012) 78

[70] J. K. Ahn *et al.* [RENO Collaboration], *Phys. Rev. Lett.* 108 (2012) 191802

[71] F. P. An *et al.* [Daya Bay Collaboration], *Chinese Phys.* C37 (2013) 011001

[72] T. Nakaya [T2K Collaboration], talk presented at Neutrino 2012

[73] P. Adamson *et al.* [MINOS Collaboration], *Phys. Rev. Lett.* 107 (2011) 181802

[74] E. K. Akhmedov, R. Johansson, M. Lindner, T. Ohlsson and T. Schwetz, *JHEP* 0404 (2004) 078

[75] M. Batygov, S. Dye, J. Learned, S. Matsuno, S. Pakvasa and G. Varner, arXiv:0810.2580 [hep-ph]; P. Ghoshal and S. T. Petcov, *JHEP* 1103 (2011) 058 ; S. -F. Ge, K. Hagiwara, N. Okamura and Y. Takaesu, arXiv:1210.8141 [hep-ph]